Oxygen Activation

Activation of Molecular Oxygen by Anionic Gold Clusters**

Alex P. Woodham, Gerard Meijer, and André Fielicke

Nano- and sub-nanoparticle materials have been the subject of much recent theoretical and experimental study owing to their novel physical and chemical properties, often quite unlike those of the bulk phase. Perhaps some of the most investigated systems are those of the gold nanoparticles which demonstrate a remarkable catalytic activity, notably towards low-temperature oxidation reactions involving molecular oxygen as first observed by Haruta et al.[1]

Unlike other transition-metal oxidation catalysts, which typically perform oxidation by the Mars-van-Krevelen mechanism,[2] formation of the key O^{2-} intermediate is thermodynamically prohibited on gold and the mechanism by which gold nanoparticles activate O_2 remains unclear. Furthermore, depending on the system, rather different mechanisms may be relevant; for example, the catalytic activity of small Au clusters deposited on MgO substrates towards CO oxidation has been found to depend on the ability of the system to transfer electrons into the Au clusters, making them negatively charged.[3] Other findings suggest that the activation of O_2 on deposited Au particles occurs at the three-phase boundary between the Au cluster, the metal oxide, and the gas phase.[4] One experimentally fruitful approach to model this multiphase system has been to exploit the well-defined environments and experimentally and theoretically tractable sizes of small gas-phase clusters, which have themselves been observed to catalyze oxidation reactions with molecular O_2.[5]

The naturally emerging questions are, how is the molecular O_2 activated and which species are involved in the oxidation mechanism? One currently accepted picture comes from the observation that only the even-sized Au cluster anions react with O_2, and then only bind a single O_2 per cluster.[6] This reactivity has been correlated to the alternating electron affinities[7] of the gold clusters which arise from their alternating closed- and open-shell electronic structure. It is therefore assumed that the activation of O_2 is through single-electron donation from the anionic cluster into the $O_2 \pi^*$ orbital, which is antibonding in nature, and thus the O—O bond is weakened forming a superoxo (O_2^-) moiety upon complexation. This picture has also been confirmed by

theoretical studies.[8] Some of the $Au_kO_2^-$ complexes ($k \leq 7$) have been further characterized by anion photoelectron spectroscopy (PES) and although vibrational substructures have been observed these only lead to insights into the final state of the detachment process, that is, the neutral complex.[9] The PES spectra reveal that on small, odd-numbered Au cluster anions O_2 is essentially molecularly physisorbed.[9c] Significant differences in the reactivities towards O_2 have been used to discriminate between different isomers of gold cluster anions up to Au_{18}^-.[10]

As the activation of the O_2 molecule upon complexation changes the bond order this process can be sensitively probed using vibrational spectroscopy. For instance, free O_2 has a stretching frequency of 1556 cm^{-1} while electron transfer into the π^* orbital successively lowers this frequency to 1074 cm^{-1} for a superoxo, O_2^-, or 866 cm^{-1} for a peroxo, O_2^{2-}, species.[11] Herein we analyze the bonding of O_2 in the complexes formed with anionic gold clusters using infrared multiple-photon dissociation (IR-MPD) spectroscopy. All the experiments reported were performed using a molecular beam apparatus housed at the "Free Electron Laser for Infrared eXperiments" (FELIX) facility[12] in Nieuwegein, the Netherlands. Full details of the machine can be found elsewhere[13] but in summary clusters are formed by laser ablation from a solid target rod of gold and reacted at approximately 173 K with molecular O_2 which is pulsed into the reaction channel attached to the cluster source block. The IR spectra of the complexes are measured mass selectively by recording the changes in their mass spectrometric intensity as a function of the IR excitation frequency, that is, by depletion spectroscopy. In these experiments we covered the range from 700 to 1400 cm^{-1} to include the regions where activated O_2 (O_2^- and O_2^{2-}) would be expected to absorb, however, for all complexes investigated bands are only observed between 1000 and 1100 cm^{-1}.

Figure 1 shows the IR-MPD spectra recorded for each of the even-sized anionic gold-cluster oxygen complex mass channels ($Au_{2n}O_2^-$; $n = 2$–7,9,10). The spectra are obtained from parent depletion spectra and then power normalized to yield a relative cross section. These were the only clusters in the size range investigated to show binding of O_2, in agreement with previous studies.[6,7,9a,14] The non-observation of a Au_{16}^- cluster complex is also in agreement with previous studies and has been attributed to the spherical aromaticity of the cage-like Au_{16}^- which gives rise to an anomalously high electron affinity (EA) and therefore unfavorable electron donation.[15] For all the $Au_{2n}O_2^-$ complexes the IR-MPD spectra show a band in a narrow range around 1060 cm^{-1}. This is a characteristic value for an O–O stretch of a superoxo moiety and can be assigned as such given that no other vibrational fundamentals are expected at this frequency.

[*] A. P. Woodham, Prof. Dr. G. Meijer, Dr. A. Fielicke
Fritz-Haber-Institut der Max-Planck-Gesellschaft
Faradayweg 4–6, 14195 Berlin (Germany)
E-mail: fielicke@fhi-berlin.mpg.de

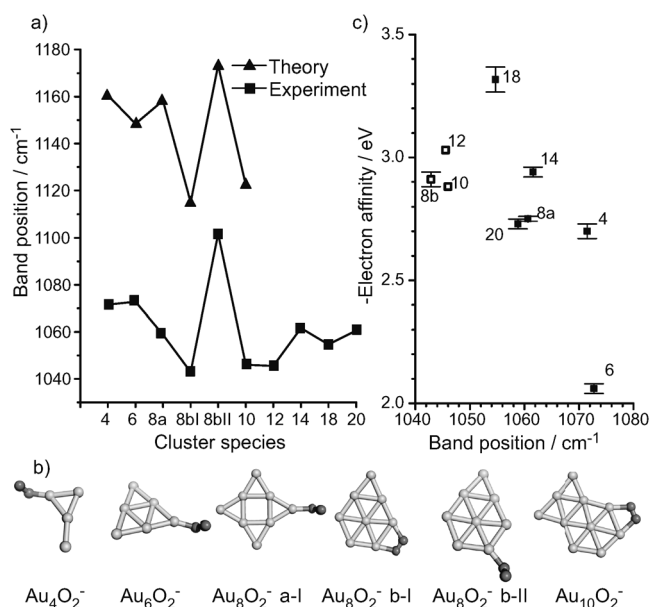Supporting information for this article is available on the WWW under http://dx.doi.org/10.1002/anie.201108958.
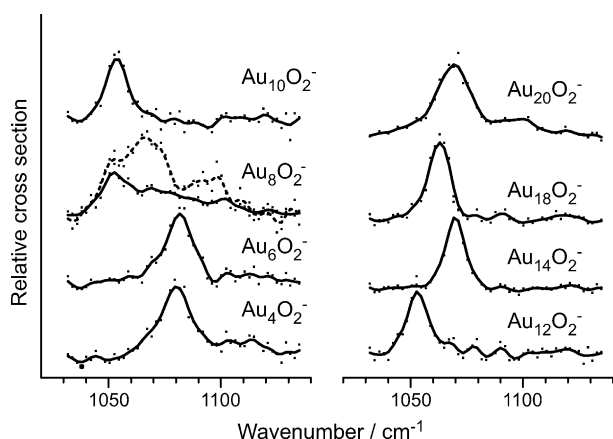
Figure 1. IR-MPD spectra of even-sized gold-cluster oxygen complexes, $Au_{2n}O_2^-$. The traces are a five-point binomially weighted running average of the raw data points (black dots). For $Au_8O_2^-$ two traces are shown, one continuous the other dashed and are intended to emphasize the different features observed in the spectra under different source conditions, see text.

Figure 2. a) Comparison of the theoretically predicted and the experimentally observed O—O stretching frequencies. The connecting lines are given as a guide for the eye. The experimental error of the frequencies is estimated to be on the order of ± 3 cm^{-1}. b) The structures corresponding to the putative global minima and two additional isomers for $Au_8O_2^-$. c) Correlation between electron affinities of the gold clusters and the experimentally determined $\nu(O-O)$ values. 8b-II is not included as it is assumed to be an intermediate structure. For Au_{10}^- we have used an estimated EA based on the DFT calculations, see Supporting Information. The labels indicate which cluster (and isomer) the data refer to. Open squares are μ^2 type binding, closed μ^1.

With the exception of $Au_8O_2^-$ all the spectra show only a single, relatively narrow (ca. 15 cm^{-1} full width at half maximum) feature with a maximum depletion of approximately 80% of the initially observed signal intensity. The exact position of this band depends on the cluster size and varies by around ± 20 cm^{-1}, although there does not appear to be a smooth monotonic trend with size, as for instance seen in the stretching frequency of CO bound to charged transition-metal clusters.[16] The general trend with growing cluster size is for $\nu(O-O)$ to decrease until a minimum around $Au_{10}O_2^-$ and $Au_{12}O_2^-$ before $\nu(O-O)$ increases again until $Au_{20}O_2^-$ which is the largest size studied (Figure 2a).

$Au_8O_2^-$ is somehow special; a broader feature is seen which appears to be composed out of multiple (apparently three), poorly resolved bands. The detailed shape of the band envelope sensitively depends on the cluster source and reaction conditions. As examples, two spectra are shown for $Au_8O_2^-$ with the first one (Figure 1, continuous line) highlighting the most red-shifted peak centered at 1043 cm^{-1} and the second (Figure 1, dashed line) emphasizing the two features blue shifted with respect to the first one, at 1059 cm^{-1} and 1102 cm^{-1}. The sum of the depletions for all three features is greater than 100%, indicating interconversion between the isomers on the μs timescale of the experiment. The two different spectra correspond to slightly different O$_2$ and He carrier-gas backing pressures which appear to sensitively influence the identity of the reacting gold clusters, the structure of the formed complexes with O$_2$, or perhaps even both.

To obtain a more detailed insight into the O$_2$ binding geometries and to resolve the origin of the different features in the $Au_8O_2^-$ spectra, a series of density functional theory (DFT) calculations was performed on the smallest cluster sizes ($Au_{2n}O_2^-$; $n = 2-5$), the results of which are summarized in Figure 2. The calculations were performed using the TURBOMOLE v6.2 package[17] employing the TPSSh[18] functional with the def2-TZVP[19] basis set and a scalar relativistic potential for the core electrons of the Au atoms. Many starting geometries were tried using the ground and low-lying isomer structures from previous studies[10b,c,20,21] as a basis for generating the oxygen complexes. The resulting putative ground-state structures are given in Figure 2b and reveal two different binding motifs for O$_2$: bridging (μ^2) and nonbridging (μ^1). The smaller clusters ($n = 2,3$) favor μ^1 whilst the larger clusters ($n = 4,5$) prefer μ^2. Figure 2a shows the calculated $\nu(O-O)$ frequencies and the experimental ones. Qualitatively the agreement is good with an almost uniform offset of approximately 80–90 cm^{-1} between theory and experiment, lending weight to the validity of the calculations. Additional information, including higher energy isomers, can be found in the Supporting Information.

The structure of $Au_4O_2^-$ is similar to the reported one[9b] with the O$_2$ binding to a two-coordinate Au apex atom. In $Au_6O_2^-$ a similar binding is found. $Au_8O_2^-$ is discussed in more detail below. For the pure Au_{10}^- metal cluster, several isomers have been identified before by anion PES in combination with O$_2$ titration, resulting in the conclusion that the most stable Au_{10}^- isomer (D_{3h}) is not reactive towards O$_2$.[10c,21] We observe this in our mass spectrum, as Au_{10}^- shows significantly less conversion into the oxygen complex and thus the spectra reported herein are dominated by the (small) fraction of reactive Au_{10}^- isomers. The lowest energy structure of $Au_{10}O_2^-$ we identify corresponds to a cluster isomer which is

not amongst the ones reported by Huang and Wang.[10c,21] It is, however, formed upon attachment of O_2 to several of the energetically low-lying isomers reported by them and further relaxation of these species. Whilst the O_2 complexes of the other planar Au_{10}^- structures are local minima, their O–O stretch typically appears at significantly higher frequencies than our assigned structure (e-I) although other only slightly higher lying isomers (d-I and d-III, in the Supporting Information) cannot be ruled out. As there are no other features in the IR-MPD spectrum of $Au_{10}O_2^-$ this suggests that all these complexes relax into a single structure. $Au_{12}O_2^-$ shows a band very close to that of $Au_{10}O_2^-$ and it may be assumed that there is a similar O_2 binding geometry, involving a seven Au atom hexagonal motif, which is present for the planar isomer of $Au_{12}^{-[22]}$ and a complex very similar to the ones seen for $Au_{10}O_2^-$ or $Au_8O_2^-$ b-I can be formed from this species. For this size and the larger clusters, however, we have refrained from additional calculations. For the larger sizes the O–O stretching frequency increases. Neither Au_{14}^- nor Au_{20}^- are expected to possess the hexagonal motif observed in the Au_8^- to Au_{12}^- clusters and thus are expected to prefer an apex-binding mode, similar to that observed for $Au_4O_2^-$ and $Au_6O_2^-$, as predicted by Molina and Hammer for $Au_{20}O_2^-$.[23]

For $Au_8O_2^-$ we experimentally observe a more complicated band structure, suggesting the presence of multiple isomers. From anion PES two isomers have been identified before, a planar star-shaped D_{4h} symmetric one (8a) and an edge-capped hexagon of C_{2v} symmetry (8b). The C_{2v} isomer has been reported to be more reactive towards O_2.[10b] This result is in agreement with our finding of a μ^2 complex of 8b (isomer 8b-I) being the overall lowest energy configuration for $Au_8O_2^-$, with the 8a-I complex predicted to lie 0.11 eV higher in energy and 8b-II 0.30 eV higher than that. Of all the structures calculated these three isomers also show the highest O_2 binding energy, ranging from 0.98 eV for the 8b-I isomer to 0.57 eV for 8b-II. The calculated frequency for 8b-I is rather low and can be related to the most red-shifted peak in the $Au_8O_2^-$ spectrum. Isomer 8b-II, which can be viewed as a precursor to the formation of the more stable b-I isomer, but with a μ^1 bound O_2 has a ν(O–O) signal approximately 60 cm^{-1} higher in frequency, which agrees with the width of the experimentally observed band pattern. For the second Au_8^- isomer the most stable O_2 complex (8a-I) shows a μ^1 O_2 bound to the two-coordinate apex atom, similar to the smaller $Au_{2n}O_2^-$ complexes. Such a structure is predicted to give a ν(O–O) which lies between those of the two 8b complexes and is only slightly too high for the experimentally observed middle feature.

The next question is whether the variations in ν(O–O) are, at least in part, determined by the electronic structure of the bare gold clusters? Electron affinities (EAs) are an easily accessible measure of this and Figure 2c shows a plot of the experimentally observed EAs (taken from Refs. [10,21,24]) as a function of the observed ν(O–O) frequency. For Au_{10}^- we instead use a calculated vertical detachment energy (VDE) for the Au_{10}^- parent isomer corresponding to the minimum energy structure of $Au_{10}O_2^-$ as an experimental EA is not known (for details see the Supporting Information). For the nonbridging complexes (μ^1) we find an approximate anti-correlation between the EA and ν(O–O), that is, those clusters with a low EA show a stronger O–O bond and thus a high ν(O–O). Such an observation is perhaps counterintuitive as it would be expected that those gold clusters with a lower EA are more likely to donate this electron density into the O_2 π^* orbital, and give a weaker O–O bond and a lower ν(O–O). According to Koopmans' theorem the EA of a species is a measure of the energy of its HOMO, ε_{HOMO}. A low EA corresponds to a higher lying HOMO, and thus a larger energy separation between it and the energetically much lower O_2 π^* orbital (as IE$(O_2) \gg$ EA(Au_n)), that is, larger $|\varepsilon_{HOMO} - \varepsilon_{\pi^*}|$. When $|\varepsilon_{HOMO} - \varepsilon_{\pi^*}|$ is large, the extent of overlap between the gold cluster HOMOs and the O_2 π^* orbital is reduced, and thus less electron density is transferred into the O_2 π^* orbital, resulting in the observed stronger O–O bond, and a higher ν(O–O). Such a picture corresponds to a molecular variant of the Newns–Anderson binding model which has been used to rationalize the reactivities of noble-metal surfaces with a variety of small ligands.[25] Indeed it has also been shown by Hoffmann[26] that such density of states (DOS) models are intimately related to frontier orbital models, and thus applicable to the present discussion. Under this DOS model, as the energy separation between the metallic d-bands and the adsorbate orbitals increases the resultant states, which are of cluster–O_2 antibonding character, begin to rise above the Fermi level. This change has two effects, firstly, the aforementioned reduction in electron donation into the O_2 π^* orbital and concomitant strengthening of the O–O bond, secondly the cluster–O_2 interaction is expected to strengthen, in agreement with reported reactivites[7] in which Au_4^- and Au_6^- are the most reactive towards O_2 binding, despite, in the present work, showing the smallest activation of the O–O bond.

In summary we have presented IR-MPD spectra of anionic gold-cluster O_2 complexes and show direct experimental evidence for the formation of a superoxo moiety upon O_2 complexation. The frequency of the ν(O–O) vibration, and thus the extent of activation, can be approximately anti-correlated with the EA of the gold cluster. This result is in contrast with the direct correlation previously established for the reactivities of the gold anions with O_2 and results in a picture of the more reactive species leading to less activation of O_2 which may have some bearing in future understanding of nano-sized gold catalysis.

[1] M. Haruta, N. Yamada, T. Kobayashi, S. Iijima, _J. Catal._ **1989**, _115_, 301–309.

[2] P. Mars, D. van Krevelen, _Chem. Eng. Sci._ **1954**, _3_, 41–59.

[3] a) V. Simic-Milosevic, M. Heyde, X. Lin, T. König, H.-P. Rust, M. Sterrer, T. Risse, N. Nilius, H.-J. Freund, L. Giordano, G. Pacchioni, _Phys. Rev. B_ **2008**, _78_, 235429; b) B. Yoon, H. Häkkinen, U. Landman, A. S. Wörz, J.-M. Antonietti, S.

Abbet, K. Judai, U. Heiz, *Science* **2005**, *307*, 403–407; c) A. Sanchez, S. Abbet, U. Heiz, W.-D. Schneider, H. Häkkinen, R. N. Barnett, U. Landman, *J. Phys. Chem. A* **1999**, *103*, 9573–9578.

[4] I. X. Green, W. Tang, M. Neurock, J. T. Yates, *Science* **2011**, *333*, 736–739.

[5] a) L. D. Socaciu, J. Hagen, T. M. Bernhardt, L. Wöste, U. Heiz, H. Häkkinen, U. Landman, *J. Am. Chem. Soc.* **2003**, *125*, 10437–10445; b) S. M. Lang, T. M. Bernhardt, R. N. Barnett, B. Yoon, U. Landman, *J. Am. Chem. Soc.* **2009**, *131*, 8939–8951; c) S. M. Lang, T. M. Bernhardt, R. N. Barnett, U. Landman, *J. Phys. Chem. C* **2011**, *115*, 6788–6795.

[6] D. M. Cox, R. Brickman, K. Creegan, A. Kaldor, *Z. Phys. D* **1991**, *19*, 353–355.

[7] B. Salisbury, W. Wallace, R. Whetten, *Chem. Phys.* **2000**, *262*, 131–141.

[8] a) L. M. Molina, B. Hammer, *J. Chem. Phys.* **2005**, *123*, 161104; b) G. Mills, M. S. Gordon, H. Metiu, *Chem. Phys. Lett.* **2002**, *359*, 493–499.

[9] a) D. Stolcic, M. Fischer, G. Ganteför, Y. D. Kim, Q. Sun, P. Jena, *J. Am. Chem. Soc.* **2003**, *125*, 2848–2849; b) Q. Sun, P. Jena, Y. D. Kim, M. Fischer, G. Ganteför, *J. Chem. Phys.* **2004**, *120*, 6510–6515; c) W. Huang, H.-J. Zhai, L.-S. Wang, *J. Am. Chem. Soc.* **2010**, *132*, 4344–4351.

[10] a) W. Huang, S. Bulusu, R. Pal, X. C. Zeng, L.-S. Wang, *ACS Nano* **2009**, *3*, 1225–1230; b) W. Huang, R. Pal, L.-M. Wang, X. C. Zeng, L.-S. Wang, *J. Chem. Phys.* **2010**, *132*, 054305; c) W. Huang, L.-S. Wang, *Phys. Chem. Chem. Phys.* **2009**, *11*, 2663–2667.

[11] K. Huber, G. Herzberg, *Constants of Diatomic Molecules NIST Chemistry WebBook*, *NIST Standard Reference Database Number 69*, P. Linstrom, W. Mallard, National Institute of Standards and Technology.

[12] D. Oepts, A. van der Meer, P. van Amersfoort, *Infrared Phys. Technol.* **1995**, *36*, 297–308.

[13] A. Fielicke, G. von Helden, G. Meijer, D. B. Pedersen, B. Simard, D. M. Rayner, *J. Phys. Chem. B* **2004**, *108*, 14591–14598.

[14] J. Hagen, L. D. Socaciu, M. Elijazyfer, U. Heiz, T. M. Bernhardt, L. Wöste, *Phys. Chem. Chem. Phys.* **2002**, *4*, 1707–1709.

[15] S. Bulusu, X. Li, L. S. Wang, X. C. Zeng, *Proc. Natl. Acad. Sci. USA* **2006**, *103*, 8326–8330.

[16] A. Fielicke, G. von Helden, G. Meijer, D. B. Pedersen, B. Simard, D. M. Rayner, *J. Chem. Phys.* **2006**, *124*, 194305.

[17] O. Treutler, R. Ahlrichs, *J. Chem. Phys.* **1995**, *102*, 346–354.

[18] V. N. Staroverov, G. E. Scuseria, J. Tao, J. P. Perdew, *J. Chem. Phys.* **2003**, *119*, 12129–12137.

[19] a) K. Eichkorn, O. Treutler, H. Öhm, M. Häser, R. Ahlrichs, *Chem. Phys. Lett.* **1995**, *240*, 283–290; b) F. Weigend, R. Ahlrichs, *Phys. Chem. Chem. Phys.* **2005**, *7*, 3297–3305.

[20] a) H. Häkkinen, U. Landman, *Phys. Rev. B* **2000**, *62*, 2287–2290; b) J. Li, X. Li, H.-J. Zhai, L.-S. Wang, *Science* **2003**, *299*, 864–867; c) D. Schooss, P. Weis, O. Hampe, M. M. Kappes, *Philos. Trans. R. Soc. London Ser. A* **2010**, *368*, 1211–1243.

[21] L. M. Wang, R. Pal, W. Huang, X. C. Zeng, L. S. Wang, *J. Chem. Phys.* **2010**, *132*, 114306.

[22] H. Häkkinen, B. Yoon, U. Landman, X. Li, H.-J. Zhai, L.-S. Wang, *J. Phys. Chem. A* **2003**, *107*, 6168–6175.

[23] L. Molina, B. Hammer, *J. Catal.* **2005**, *233*, 399–404.

[24] a) H. Häkkinen, U. Landman, *J. Am. Chem. Soc.* **2001**, *123*, 9704–9705; b) K. J. Taylor, C. L. Pettiette-Hall, O. Cheshnovsky, R. E. Smalley, *J. Chem. Phys.* **1992**, *96*, 3319–3329.

[25] a) B. Hammer, *Top. Catal.* **2006**, *37*, 3–16; b) T. Bligaard, J. Norskov, *Electrochim. Acta* **2007**, *52*, 5512–5516.

[26] R. Hoffmann, *Rev. Mod. Phys.* **1988**, *60*, 601–628.